

CONF-790622--8

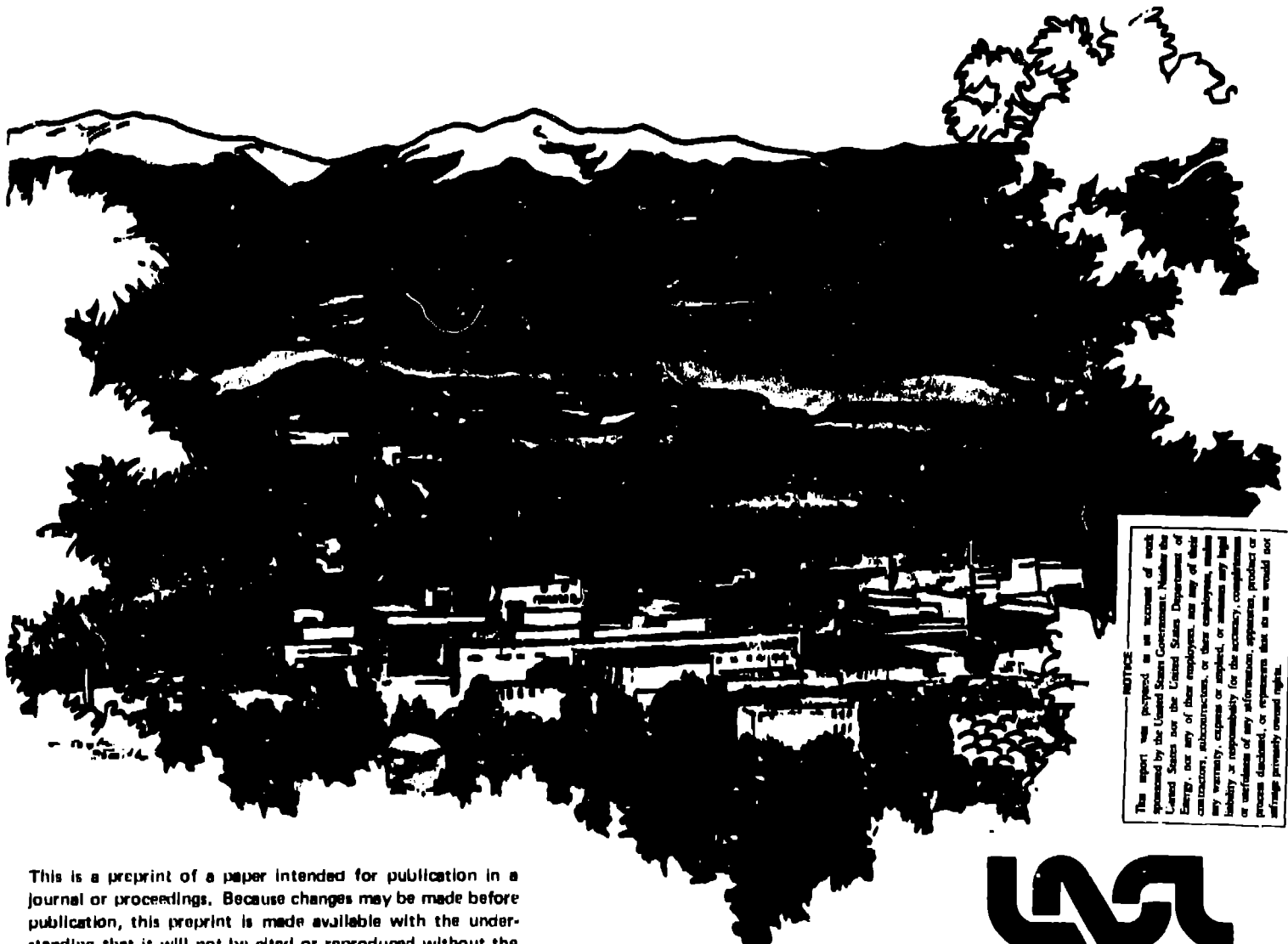
Preprint LA-UR-79-521

MASTER

Title: SIMULATIONS OF INTENSE RELATIVISTIC ELECTRON BEAM GENERATION BY FOILLESS DIODES

Author(s): MICHAEL E. JONES AND LESTER E. THODE

Submitted to: PROCEEDINGS OF THE SECOND IEEE INTERNATIONAL PULSED POWER CONFERENCE
June 11-14, 1979
Lubbock, Texas



This is a preprint of a paper intended for publication in a journal or proceedings. Because changes may be made before publication, this preprint is made available with the understanding that it will not be cited or reproduced without the permission of the author.



DISTRIBUTION OF THIS DOCUMENT IS UNLIMITED

SIMULATIONS OF INTENSE RELATIVISTIC ELECTRON BEAM GENERATION BY FOILLESS DIODES

MICHAEL E. JONES AND LESTER E. THODE

Intense Particle Beam Theory Group
Los Alamos Scientific Laboratory
Los Alamos, New Mexico 87545

Abstract

Foilless diodes used to produce intense annular relativistic electron beams have been simulated using the time-dependent, two-dimensional particle-in-cell code CCUBE. Current densities exceeding 200 kA/cm^2 have been obtained in the simulations for a 5 MeV, 35Ω diode. Many applications, including microwave generation, collective ion acceleration and high-density plasma heating require a laminar electron flow in the beams. The simulation results indicate that foilless diodes immersed in a strong external magnetic field can achieve such a flow. Diodes using technologically achievable magnetic field strengths ($\sim 100 \text{ kG}$) and proper electrode shaping appear to be able to produce beams with an angular scatter of less than 35 mrad at the current densities and energies mentioned above. Scaling of the impedance and temperature of the beam as a function of geometry, magnetic field strength and voltage is presented.

Introduction

Foilless diodes may be used for the production of intense annular relativistic electron beams for many applications including microwave generation, collective ion acceleration and high-density plasma heating.¹ Conventional foil diodes have been found to suffer from an impedance collapse when plasma, generated by electrons striking the anode foil, propagate from the anode to the cathode thereby electrically shorting the diode. This problem is eliminated by using a foilless diode, thus allowing higher current densities than can be obtained with a foil diode. In addition, the electron beam generated by a foilless diode is not perturbed by passing through a foil nor is it necessary to replace a foil for repeated operation.²

Although there has been some investigation of relativistic electron beam generation by foilless diodes a firm understanding of the diode has been

lacking.²⁻⁸ We have analyzed the simple diode illustrated in Fig. 1 to determine the scaling of diode impedance and beam temperature as a function of geometry, magnetic field strength and voltage. Some investigators have assumed that the foilless diode impedance is determined by the maximum current allowed by space charge in the drift tube. Our analysis indicates that the diode impedance is determined by the equilibrium that the beam obtains which is not necessarily the equilibrium which gives the space-charge limiting current.

Impedance Model

Because most applications require a beam with laminar flow it is useful to model the beam formed by the foilless diode by the cold fluid equations. In an azimuthally symmetric, axially homogeneous equilibrium, the equations describing the beam depend only on the radial coordinate, r . The equations to be solved are

$$mc^2/e \gamma \beta_\theta^2/r = E_r + \beta_\theta B_z - \beta_z B_\theta \quad (1)$$

$$dB_z/dr = 4\pi n e \beta_\theta \quad (2)$$

$$d(rB_\theta)/dr = -4\pi n e r \beta_z \quad (3)$$

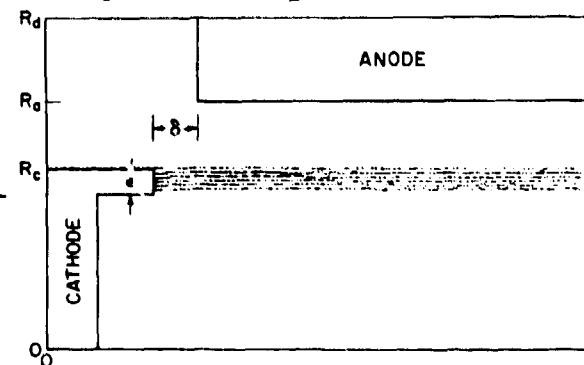


Fig. 1. Typical Foilless Diode.

$$\frac{d(rE_r)}{dr} = -4\pi n e r \quad (4)$$

where m and e are the mass and charge of the electron. The only nonzero fluid variables are the density n and the axial and azimuthal fluid velocities β_z and β_θ (divided by the speed of light c). The nonzero fluid variables are the radial electric field E_r , the azimuthal magnetic field B_θ , and the axial magnetic field B_z . The relativistic factor is denoted by γ . Because the cathode is an equipotential surface, conservation of energy assumes the following form:

$$\frac{d\gamma}{dr} = -eE_r/mc^2 \quad (5)$$

Because there are only five equations and six unknowns another condition must be specified. A condition which leads to an analytically tractable solution of the equilibrium equations and which becomes increasingly better satisfied at larger energies, is to choose β_z to be independent of r .⁹ Defining the following quantities $\gamma_{||} \equiv (1 - \beta_z^2)^{-\frac{1}{2}}$ and $\gamma_1 \equiv \gamma/\gamma_{||}$ an equation for γ_1 can be found whose solution is given in terms of elliptic Jacobi functions.⁹ The total beam current v , measured in units of mc^3/e is given by this model as

$$v = [(\gamma_{||}^2 - 1)(\gamma_{10}^2 - 1)(\gamma_{10}^2 + a^2)]^{\frac{1}{2}}/2 \quad (6)$$

where γ_{10} is γ_1 evaluated at the outside edge of the beam, R_o , and a is an arbitrary constant. Defining $w_{co} \equiv eB_z(R_o)/mc^2$ we find

$$R_o w_{co}/c = (\gamma_{10}^2 - 1)^{\frac{1}{2}} + \gamma_{10}(\gamma_{10}^2 + a^2)^{\frac{1}{2}} \quad (7)$$

$$\text{and } \ln R_o/R_i = F(\phi, k)/(a^2 + 1)^{\frac{1}{2}} \quad (8)$$

where R_i is the inside beam radius, $\phi = \cos^{-1}(\gamma_o^{-1})$ and $k = a/(a^2 + 1)^{\frac{1}{2}}$ and $F(\phi, k)$ is the incomplete elliptic integral of the second kind.

In addition to Eqs. (6)-(8), we require that the total energy of the electrons, kinetic and potential, be equal to the potential drop between the anode and cathode. This,

$$\gamma_a = \gamma_{||} \gamma_{10} + 2v/\beta_z \ln R_a/R_o \quad (9)$$

where R_a is the anode radius as (see Fig. 1). The relativistic factor that the electrons would have

upon reaching the anode is denoted by γ_a . Voronin, et al. have used these equations and additional assumptions to find the space-charge limited current as a function of magnetic field.⁸ However, there is no a priori reason to assume that the beam produced by the diode will be launched into an equilibrium which will transmit the maximum current.

If the applied external magnetic field penetrates the cathode then conservation of canonical angular momentum for takes the form:

$$(\gamma_{10}^2 - 1)^{\frac{1}{2}} = (R_o w_{co}/c - R_c^2 w_c/R_o c)/2 \quad (10)$$

where $w_c = eB_0/cm^2$ and B_0 is the applied magnetic field. The cathode radius is denoted by R_c . If in addition we assume that the laminar electron flow is along the self-consistent magnetic field lines, then the flux between the axis and the outer edge of the beam is equal to the applied flux between the axis and the cathode radius. On the time scale of most experiments, the magnetic field produced by the beam cannot diffuse through the anode wall. Therefore, the flux between the outer edge of the beam and the anode will be equal to the applied flux between the cathode and anode. These conditions may be written as

$$R_c^2 w_c/c = 2 R_o (\gamma_{10}^2 - 1)^{\frac{1}{2}} + R_i (1 + a^2)^{\frac{1}{2}} \quad (11)$$

$$\text{and } w_{co}(R_a^2 - R_o^2) = w_c(R_a^2 - R_c^2) \quad (12)$$

Equations (6)-(12) form a complete set of equations which can be solved (numerically) to determine the impedance of the foilless diode. In order to insure laminar flow, it is necessary to apply a large external magnetic field, therefore, a useful approximation can be obtained by taking the infinite magnetic field limit. One then finds that the beam becomes infinitesimally thin with radius R_c and that the beam approaches a nonrotating equilibrium. The diode impedance in this limit becomes

$$Z = 15(\gamma_a - 1)\{[\gamma_a/(1 + 4 \ln R_a/R_c)]^2 - 1\}^{-\frac{1}{2}} \Omega. \quad (13)$$

It should be noted that this formula is invalid for low voltage, probably owing to our assumption of β_z being independent of r .

Diode Simulations

A two-dimensional relativistic time-dependent particle-in-cell simulation code, CCUBE, has been used to test the impedance model and gain insight into the parameters affecting beam quality.¹⁰ An emission algorithm in the code emits charge from the cathode surface at a sufficient rate to satisfy the space-charge limited emission boundary condition, i.e., the electric field normal at the cathode is zero. The diode simulations were run with a transverse electromagnetic (TEM) wave launched from the left in Fig. 1 onto the coaxial transmission line. By not allowing the first few cells to emit, one can control the impedance of the driver to the diode, which in all cases was taken to be 37Ω . Typically the length of the simulation region, L , was 5 to 10 cm. Impedances and beam parameters are measured when the system consisting of the transmission line driver with the diode load had reached steady state. At this time the voltage on the diode, V , is given by

$$V = 2V_w Z / (Z_0 + Z) \quad (14)$$

where Z is the diode impedance, Z_0 is the transmission line impedance and V_w is the voltage of the TEM wave launched onto the line. Diagnostics in the code include voltage and particle current probes, Rogowski Coils as well as impedance probes located at several axial positions. At the end of the simulation region diagnostics include Faraday Cups, calorimeters and density, mean velocity, and temperature measurements as a function of radial position.

Simulation Results

From Eq. (13) we see that for large applied magnetic fields the diode impedance depends only on the voltage and the ratio of the anode to cathode radius. Figure 2 shows the results of several simulations performed with a $V_w = 5.1$ MV and a cathode radius, $R_c = 1$ cm. Because of the impedance mismatch, the voltage across the diode varied from 3.5 to 6.0 MV in accordance with Eq. (14). The open circles represent simulations performed with an applied magnetic field of 100 kG and an A-K gap, δ , (see Fig. 1) of 0.4 cm. The triangle represents a run with the same parameters but with $\delta = 0.2$ cm.

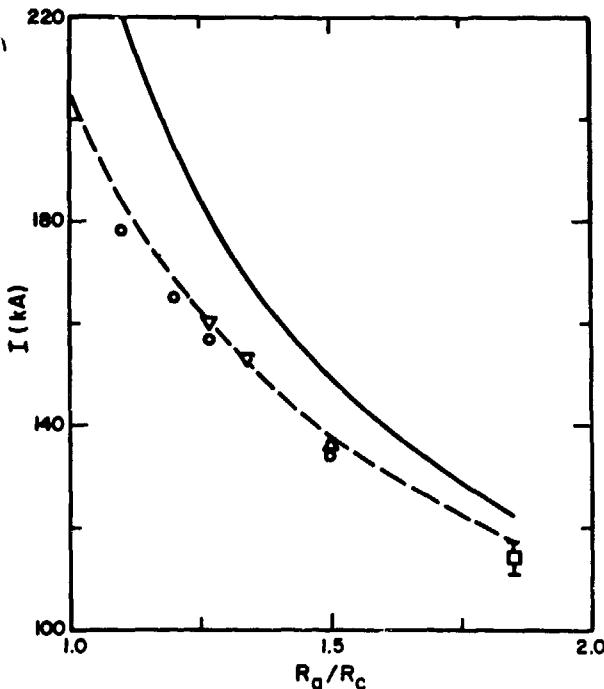


Fig. 2. Current versus ratio of anode to cathode radius for various foilless diodes. The dashed line is from Eq. (13). The solid line is the space-charge limit.

Two runs at 40 kG and $\delta = 0.4$ cm are denoted by inverted triangles. The square designates a run at 55 kG in which the anode wall is continued straight at the original transmission line radius, R_d , of 1.85 cm so that $\delta \rightarrow \infty$. The dashed line is obtained from Eq. (13). The solid line is the space limiting current for the infinitesimally thin beam in the infinite magnetic field limit.¹⁴ The simulation data in all cases lies well below the space-charge limiting current and rather close to the current given by the impedance formula of Eq. (13). All the simulations were performed with a cathode tip thickness, ϵ in Fig. 1, of 0.135 cm except the run at 55 kG which had ϵ equal to R_c . At 100 kG the beam thickness was found to be approximately 0.03 cm, thus it is unlikely that much effect would be found for ϵ 's larger than this value. These very thin beams can yield current densities exceeding 700 kA/cm^2 .

Because Eq. (13) was obtained for the infinite magnetic field limit, it is desirable to determine the effects of finite magnetic field. Figure 3 shows the results of a series of simulations performed with $V_w = 5.1$ MV, $R_a = 1.27$ cm, $\delta = 0.4$ cm,

and $\epsilon=0.135$ cm. The dashed curve is obtained from the numerical solution of Eqs. (6)-(12). The solid curve is the space-charge limited diode theory of Voronin, et al.¹⁰ The diode operates well below the space-charge limit and again agrees well with the laminar flow impedance model. The beam strikes the anode wall at 25 kG and for all values of applied field below this value the transmitted electron current gradually diminishes owing to current loss to the anode. Although the diode impedance does not vary much with magnetic field, the temperature as measured by the mean annular scatter of electrons around the beam propagation direction was found from the simulations to vary from 200 mrad at 27 kG to less than 60 mrad at 100 kG. The high magnetic field makes it more difficult for the electrons to cross field lines and create temperature by mixing.

One would expect that as δ is increased to larger values that the beam produced by the foilless diode would come to equilibrium before it "sees" the reduced anode radius R_a . The existence of this effect is verified by the series of simulations shown in Fig. 4. The parameters of the simulations include $B_0=100$ kG, $V_w=5.1$ MV, $R_d=1.5$ cm, and $\epsilon=0.135$ cm. The upper dashed curve was calculated from Eq. (13). The lower dashed curve was also calculated from Eq. (13) but with R_a equal to outer radius of the transmission line feed R_d . As seen from the data, the diode impedance makes a sudden transition from an equilibrium with an anode radius of R_a for small δ to an equilibrium with anode radius R_d at large δ . The value of δ at the transition point is roughly one-half of the cathode radius for this case. The actual transition point is probably governed by the

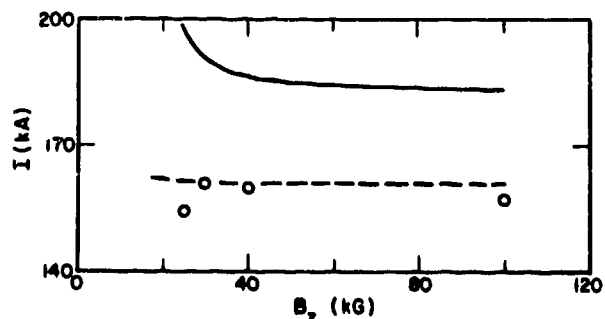


Fig. 3. The effect of finite magnetic field on diode impedance.

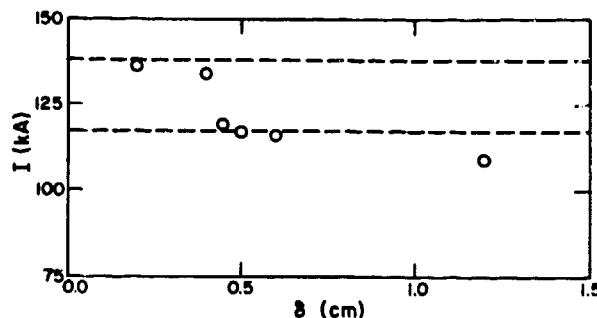


Fig. 4. Current versus A-K gap, δ , for the foilless diode.

distance the beam must propagate from the cathode tip to reach equilibrium and must certainly depend upon the current density.

For large values of δ , the beam gains kinetic energy as it approaches the region in which the anode radius is reduced to R_a making it stiffer and less likely to phase mix. Simulations have shown beam temperatures below 25 mrad for this scheme, which is near the numerical resolution of the code. Use of these ideas in diode design show promise for producing very laminar beams.

References

1. L. E. Thode, Los Alamos Scientific Laboratory report LA-7169-P (February 1978).
2. M. Friedman and M. Ury, Rev. Sci. Inst. 41, 1334 (1970).
3. M. E. Read and J. A. Nation, J. Plasma Phys. 13, 127 (1975).
4. A. A. Kolomenskii, E. G. Krastelev, and B. N. Yablokov, Pis'ma Zh. Tekh. Fiz. 2, 271 (1976).
5. E. Ott, T. M. Antonsen and R. V. Lovelace, Phys. Fluids 20, 1180 (1977).
6. J. Chen and R. V. Lovelace, Phys. Fluids 21, 1623 (1978).
7. D. C. Straw and M. C. Clark, Proceeding of 1979 IEEE Particle Accelerator Conference.
8. V. S. Voronin, E. G. Krastelev, A. N. Lebedev, and B. N. Yablokov, Fiz. Plazmy 4, 604 (1978).
9. A. V. Agafonov, V. S. Voronin, A. N. Lebedev and K. N. Pazin, Zh. Tekh. Fiz. 44, 1909 (1974).
10. M. E. Jones and L. E. Thode, Los Alamos Sci. Lab. report LA-7600-MS (January 1979).
11. B. N. Brejzman and D. D. Ryutov, Nucl. Fusion 14, 873 (1974).

This work was supported by the AFOSR and DOE.